JOURNAL OF MATERIALS SCIENCE 29 (1994) 1497–1500

Morphology of polycrystalline ZnO and its physical properties

L. KOUDELKA, J. HORÁK
University of Chemical Technology, 53210 Pardubice, Czech Republic
P. JARIABKA
Slovlak, 01864 Košeca, Slovakia

Five commercial polycrystalline ZnO samples with different morphologies (nodular and needle-like) have been studied. Nodular ZnO crystallites reveal lower polydispersity, higher ultraviolet luminescence (380 nm), low green luminescence (500 nm), a small ESR signal with $g = 1.96$ and a density close to the theoretical value for ZnO with the wurtzite structure. Needle-like ZnO crystallites have a higher polydispersity, higher green luminescence, higher ESR signal with $g = 1.96$ and lower values of density. The observed differences in the physical properties are associated with the presence of oxygen vacancies in needle-like particles and probably also interstitial zinc atoms in nodular particles.

1. Introduction

Zinc oxide is produced industrially in great quantities by oxidation of zinc vapours [1]. There are several world companies which supply commercial ZnO used as a white pigment and filler for rubber products. The quality of the products is evaluated by several parameters, such as purity, whiteness, heavy metal content, etc. For the preparation of homogeneous mixtures, the morphology of ZnO particles also plays an important role. ZnO crystallizes in the hexagonal wurtzite lattice [2] and very often its crystallites have a needle-like form. On the other hand, some companies are able to produce isometric crystallites of ZnO which are advantageous for its easy dispergation in viscous media.

We have investigated the morphology, particle-size distribution and some physical properties of different ZnO samples. These studies have shown interesting correlations between morphology and some physical properties of several ZnO samples.

2. Experimental procedure

For the proposed study, several samples from different sources were chosen, as shown in Table I.

The crystalline structure was verified by X-ray diffraction using an X-ray diffractometer HZG 4B (Freiberg) and CuK_α radiation. The morphology of the ZnO particles was investigated using a scanning electron microscope, Tesla BS 301. ZnO powder was glued to the aluminium substrate and covered with gold to remove the space charge from the ZnO particles. Particle-size distribution was measured using a Sedigraph (Micromeritics) in water suspension using 0.9% Na_2HPO_4 for better dispergation. The density of the powder samples was measured using an Autopycnometer 1320 (Micromeritics).

Luminescence spectra of ZnO samples were measured on a Hitachi–Perkin–Elmer MPF-2A luminescence spectrometer; the relative intensity of the luminescence was measured against a standard sample NBI/SDI. Electron spin resonance of ZnO samples was recorded with an electron resonance spectrometer ERS 201 (AdW Berlin).

3. Results

X-ray diffraction analysis has shown that all the ZnO samples studied contain crystallites of the hexagonal wurtzite structure having nearly the same lattice parameters values for all the samples, 1–5, as $a = 0.324\,97 \pm 0.000\,02$ and $c = 0.520\,66 \pm 0.000\,03$ nm.

The morphology of the ZnO samples studied by the SEM method is shown in Fig. 1. It can be seen that the shape of ZnO crystallites in the samples 1 and 2 is nearly isometric. When the size of ZnO crystallites of samples 1 (Peru) and 2 (Pharma Grillo) are compared (see Fig. 1a, b), it can be clearly seen that the size of ZnO crystallites in the first sample is much smaller than that in the latter sample. On the other hand, samples 3–5 show the presence of needle-like crystallites. Owing to the different orientation of crystallites, the needle-like shape is evident only in some crystallites as shown in Fig. 1c–e.

TABLE I List of studied commercial polycrystalline ZnO samples

Sample	Specification
1	Peru
2	Pharma Grillo
3	Rotsiegel Grillo
4	Slovlak ZP
5	Slovlak P20

0022–2461

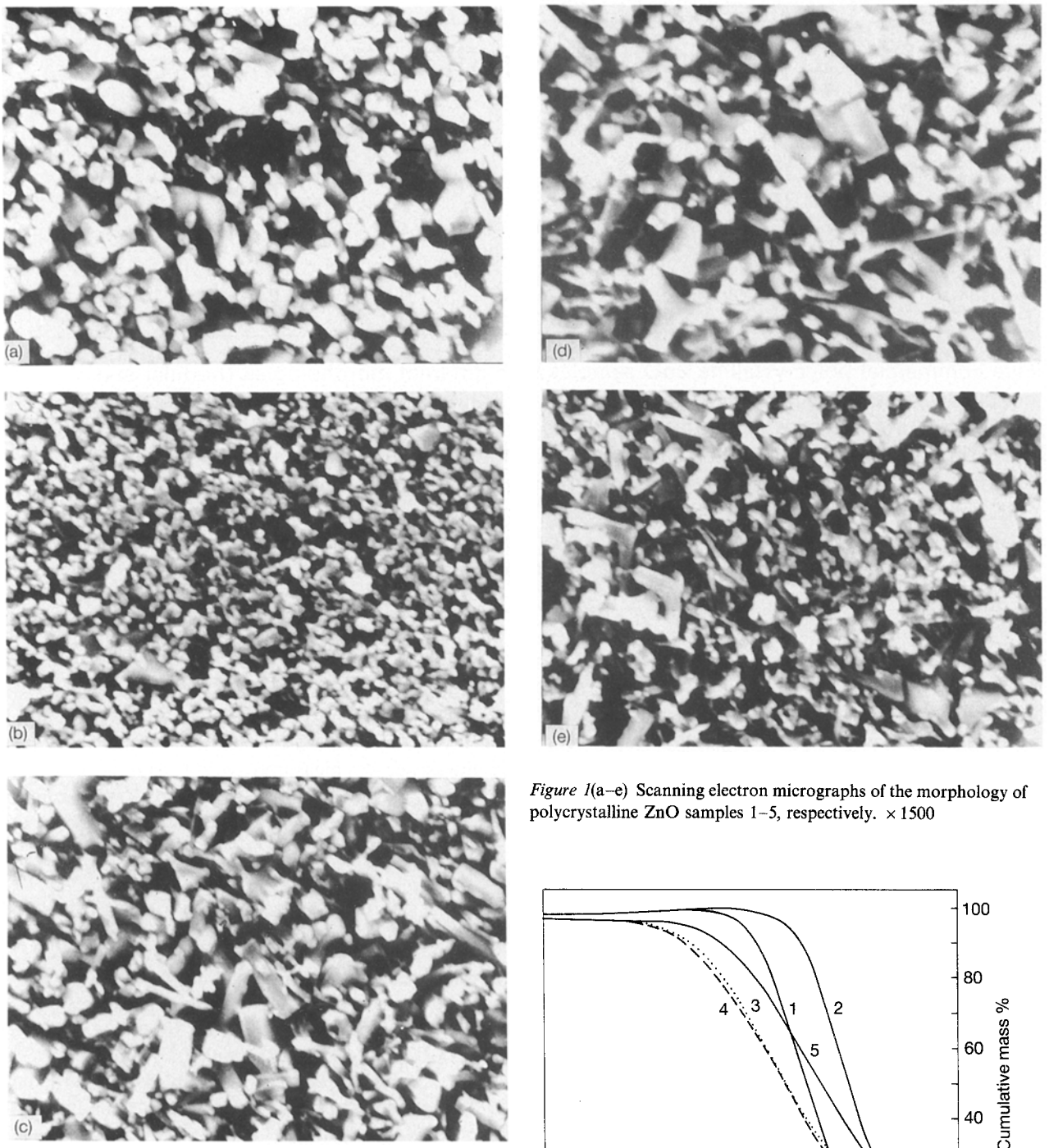

Figure 1(a–e) Scanning electron micrographs of the morphology of polycrystalline ZnO samples 1–5, respectively. × 1500

Figure 2 Particle-size distribution of polycrystalline ZnO samples determined by sedimentation analysis.

The particle-size distribution curves (Fig. 2), are in a good agreement with the results of the SEM study. The values of polydispersity, σ, were calculated as described by Batel [3] for the log-normal distribution of particles given in Table II. The first two samples, 1 and 2, reveal narrower distribution curves and smaller polydispersity than samples 3–5. The values of the medium Stokes diameter, d_{50}, obtained from the distribution curves are also given in Table II, as are powder density values. The highest density values were obtained for samples 1 and 2 with the nodular-type crystallites, whereas the values of density of samples 3–5 were lower.

Luminescent spectra of ZnO samples are shown in Fig. 3. These spectra reveal two luminescent bands with maxima at 380 nm (ultraviolet region) and 500 nm (green region). The relative intensity of these two luminescent bands differs significantly, and their ratio, I_{380}/I_{500} is given in Table II. Samples 1 and 2 exhibit a stronger ultraviolet luminescence than the green luminescence, whereas samples 3–5 reveal very strong green luminescence. In addition the electron spin resonance spectra of ZnO samples reveal remarkable differences (see Fig. 4). In all the ZnO samples, only

TABLE II Characteristic parameters of the ZnO samples studied

Sample	Crystallite form	Medium Stokes diameter, d_{50}(nm)	Polydispersity σ	Density (g cm^{-3})	Luminescence intensity ratio, I_{380}/I_{500}	Relative intensity of ESR signal (Arb. units)
1	Nodular	0.45	0.186	5.52	1.38:1	3.8×10^3
2	Nodular	0.29	0.196	5.56	9.11:1	1.36×10^3
3	Needles	0.55	0.360	5.24	1:3.17	4.38×10^3
4	Needles	0.56	0.330	5.31	1:4.16	4.09×10^3
5	Needles	0.40	0.354	5.07	1:9.1	4.7×10^3

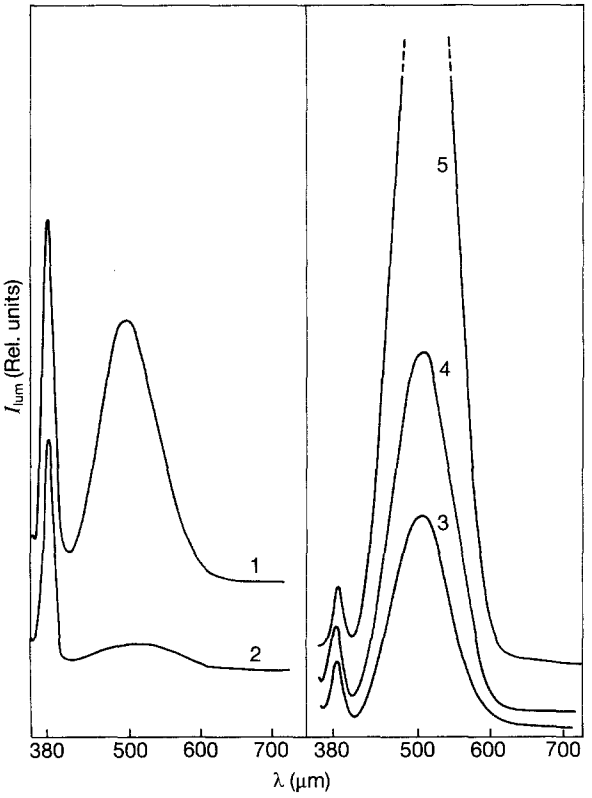

Figure 3 Luminescent spectra of polycrystalline ZnO samples.

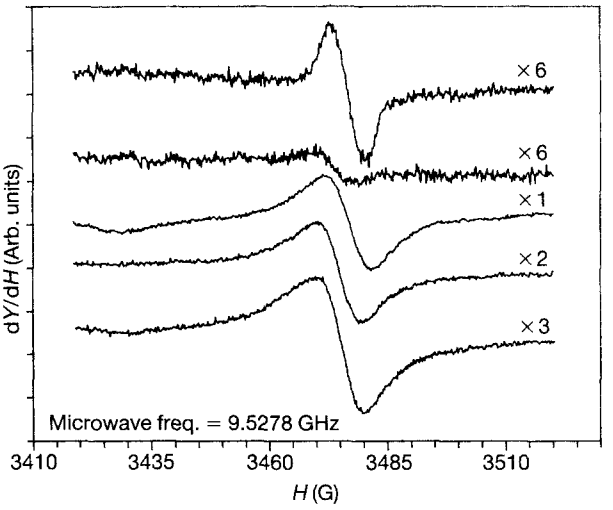

Figure 4 ESR spectra of polycrystalline ZnO samples.

one ESR signal was observed at $g = 1.9575 \pm 0.0007$. This signal has different intensities for samples 1–5 and a narrower shape for sample 1. The intensities of the ESR signals are given in Table II.

4. Discussion

The results obtained reflecting relations between morphology and properties of ZnO samples clearly show distinct differences in the properties of nodular-like particles inherent to samples 1 and 2, and those of needle-like particles inherent to samples 3–5. Nodular-type particles have a lower polydispersity than the needle-like particles. An especially great difference can be seen in the luminescence spectra (Fig. 3) which reflect different types of point defects in these two morphological groups. The nodular particles have low green luminescence intensity, peaking at 500 nm, and higher ultraviolet luminescence, peaking at 380 nm. On the other hand, the anisometric ZnO particles present in samples 3–5 reveal strong green luminescence. These differences in luminescence properties are linked to differences in point defects present in the ZnO crystals.

The ESR signal $g = 1.96$, according to Neumann [4], is caused by a donor centre because of the negative Δg. Further support for the assignment of the EPR signal to a donor centre is the vacuum or hydrogen treatment of ZnO which increases the intensity of the EPR signal and a subsequent oxygen treatment which results in an intensity decrease. According to Hausmann and Utsch [5] and Pöppl and Völkel [6] the ESR signal $g = 1.96$ can be ascribed to the single-ionized vacancy, V_O^+.

If we compare the results of the ESR study with the density values of ZnO samples (see Table II), we can see that the samples with a strong ESR signal (samples 3–5) also have lower values of density, whereas those with higher densities possess weaker ESR signals. These results support the idea that the samples with anisometric shaped ZnO particles contain oxygen vacancies because their density (5.07–5.24 g cm^{-3}) is lower than the calculated density of ZnO (5.68 g cm^{-3} [7]).

The presence of a high concentration of oxygen vacancies in needle-like ZnO samples is also supported by strong intensities of green luminescence in those samples. According to Riehl and Ortmann [8], uncharged oxygen vacancies V_O^x are responsible for the green luminescence in ZnO. Some authors [9] are convinced that the green luminescence in ZnO is caused by copper impurities incorporated in the ZnO lattice. We think that the explanation of Riehl and

Ortmann [8] is more plausible. According to our experiments, the green luminescence can be decreased by a heat treatment of polycrystalline ZnO in the reduction atmosphere. This treatment could not influence the concentration of copper atoms in the ZnO lattice. However, we cannot exclude the possibility that copper atoms may be a coactivator of the green luminescence. Thus the results of the luminescence measurement on ZnO samples provide evidence for a high concentration of uncharged oxygen vacancies V_0^x in needle-like ZnO crystals (samples 3–5) and a low concentration of V_0^x in nodular ZnO crystals (samples 1 and 2).

We assume that during the preparation of ZnO by the process of oxidation of zinc vapours by an air atmosphere according to the equation

$$\mathrm{Zn(g)} + 1/2\ \mathrm{O_2(g)} = \mathrm{ZnO(s)} \quad (1)$$

under certain conditions the formation of oxygen vacancies takes place

$$\mathrm{O} = V_0^x + 1/2\ \mathrm{O_2(g)} \quad (2)$$

The neutral oxygen vacancy, V_0^x, is occupied by two electrons and has an ionization energy $E_D = 0.02$–0.05 eV [6]; thus under the preparation conditions (1000–1400 °C [1]) it can be easily ionized according to the equation

$$V_0^x = V_0^+ + e^- \quad (3)$$

thus forming a single positively charged vacancy, V_0^+, occupied by one electron and is consequently paramagnetic and thus is manifested in the ESR measurements.

The ratio of neutral and singly charged vacancies cannot be determined, because only the concentration of charged vacancies can be found from ESR measurements (see Table II), whereas the concentration of neutral vacancies cannot be determined from the luminescence spectra.

From the results given and discussed above, we can conclude that the isometric ZnO particles are characterized by higher values of density, a low concentration of singly charged oxygen vacancies and a low concentration of uncharged oxygen vacancies. We are not convinced that the low concentration of point defects must be related to high values of density, because these data can also be influenced by the presence of zinc interstitials inside the ZnO wurtzite lattice.

From the observed relations between the morphology of ZnO particles and their physical properties, it is also possible to evaluate not only the deviation of their composition from stoichiometry, but also the technical parameters used in the production of ZnO powder by oxidation of zinc vapour. We assume that the technological process of the preparation of isometric ZnO particles is carried out in an atmosphere with an insufficient partial pressure of oxygen, and under these conditions, overstoichiometric zinc atoms enter interstitial positions inside the ZnO wurtzite lattice. Such an explanation is supported by some previously reported effects:

(a) heat treatment of ZnO powder in a reduction atmosphere decreases the intensity of the green luminescence [10] and thus decreases the concentration of oxygen vacancies; and

(b) a lower oxygen content in the system used for the vapour growth of ZnO crystals according to Yoshiie *et al.* [11] results in a decrease of the growth rate in the direction of the *c*-axis of ZnO crystals.

Acknowledgement

The authors thank Dr Zdenek Sitta, Tesla Lanškroun, for measurement of the density and particle-size distribution of the ZnO samples.

References

1. G. HÄNIG and K. H. ULBRICH, *Erzmetall* **32** (1979) 140.
2. G. HEILAND, E. MOLLWO and F. STÖCKMANN, in "Solid State Physics", Vol. 8, edited by F. Seitz and D. Turnbull (Academic Press, New York, 1959) p. 194.
3. W. BATEL, "Einführung in die Korngrössemesstechnik" (Springer, Berlin, 1971) p. 47.
4. G. NEUMANN, in "Current Topics in Materials Science", Vol. 7, edited by E. Kaldis (North-Holland, Amsterdam, 1981) p. 271.
5. A. HAUSMANN and B. UTSCH, *Z. Phys.* **B21** (1975) 217.
6. A. PÖPPL and G. VÖLKEL, *Phys. Status Solids (a)* **115** (1989) 247.
7. W. F. McCLUNE (ed). "Mineral Powder Diffraction File" (International Centre for Diffraction Data, Swarthmore, PA, 1986) Card no. 5-664, p. 1331.
8. N. RIEHL and H. ORTMANN, *Z. Elektrochem.* **60** (1956) 149.
9. H. J. SCHULZ, in "Current Topics in Materials Science", Vol. 7, edited by E. Kaldis (North-Holland, Amsterdam, 1981) p. 254.
10. E. MOLLWO, *Z. Physik* **138** (1954) 478.
11. T. YOSHIIE, H. IWANAGA, T. YAMAGUCHI and N. SHIBATA, *J. Cryst. Growth* **53** (1981) 639.

Received 7 September 1992
and accepted 27 September 1993